Monoclonal anti-MUC1 antibody with novel octahydropyrazino[2,1-a:5,4-a']diisoquinoline derivative as a potential multi-targeted strategy in MCF-7 breast cancer cells

AGNIESZKA GORNOWICZ[1], WOJCIECH SZYMANOWSKI[1], ANNA BIELAWSKA[1], ANNA SZYMANOWSKA[1], ROBERT CZARNOMYSY[2], ZBIGNIEW KAŁUŻA[3] and KRZYSZTOF BIELAWSKI[2]

Departments of [1]Biotechnology and [2]Synthesis and Technology of Drugs, Medical University of Bialystok, 15-222 Bialystok; [3]Institute of Organic Chemistry, Polish Academy of Sciences, 01-224 Warsaw, Poland

Received January 4, 2019; Accepted June 24, 2019

DOI: 10.3892/or.2019.7256

Abstract. The aim of the present study was to examine the multi-targeted potential of a monoclonal antibody against mucin-1 (MUC1) and novel octahydropyrazin[2,1-a:5,4-a'] diisoquinoline derivative (OM-86II) in estrogen receptor-positive MCF-7 human breast cancer cells. The cell viability was measured by an MTT assay. The analyses of cell cycle and disruption of mitochondrial membrane potential were performed by flow cytometry. Fluorescent microscopy and flow cytometry were used to demonstrate the effect of the compounds on apoptosis. ELISA was conducted to check the concentrations of proteins involved in multiple intracellular signaling pathways, responsible for the promotion of tumor growth and breast cancer progression, namely matrix metalloproteinase (MMP)-2, matrix MMP-9, tumor necrosis factor-α (TNF-α), cyclooxygenase-2 (COX-2), soluble intercellular adhesion molecule 1 (sICAM1) and mTOR. The combination therapy based on anti-MUC1 antibody and novel OM-86II inhibited the proliferation of MCF-7 breast cancer cells. Its inhibitory effects were associated with the induction of cell cycle arrest and apoptosis. It was demonstrated that anti-MUC1 antibody with OM-86II decreased the concentrations of MMP-2, MMP-9, sICAM1 and mTOR. In addition, the combined therapy exhibited anti-inflammatory activity, which was demonstrated by a decrease in TNF-α and COX-2 concentrations. The present data provided evidence that the combination of anti-MUC1 antibody with novel OM-86II represents a multi-targeted strategy in MCF-7 breast cancer treatment.

Correspondence to: Dr Agnieszka Gornowicz, Department of Biotechnology, Medical University of Bialystok, Kilinskiego 1, 15-222 Bialystok, Poland
E-mail: agnieszka.gornowicz@umb.edu.pl

Abbreviations: COX-2, cyclooxygenase-2; ECM, extracellular matrix; ER, estrogen receptor; MMP-2, matrix metalloproteinase-2; MMP-9, matrix metalloproteinase-9; MUC1, mucin-1; sICAM1, soluble intercellular adhesion molecule 1; TNF-α, tumor necrosis factor-α

Key words: MUC1, breast cancer, apoptosis, cell cycle, combined therapy, diisoquinoline derivatives

Introduction

Breast cancer represents the leading cause of death in women worldwide and has a poor prognosis. Estrogen and estrogen receptors (ERs) play key roles in breast cancer progression. Previous studies have demonstrated that ER is expressed in 75% of breast cancer overall (1-3). Conventional cytotoxic chemotherapy is still one of the key elements of therapeutic armamentarium, but the effectiveness of treatment is limited.

Mucin-1 (MUC1) is a transmembrane glycoprotein abnormally overexpressed in a wide range of human epithelial cancer types, including colon, breast, ovarian and pancreatic cancer (4,5). MUC1 is localized only on the apical membrane and functions via barrier formation and monitoring luminal events in healthy cells (4). Overexpression and aberrant glycosylation of MUC1 in cancer cells contribute to tumor progression and metastasis (6). MUC1 is also a heterodimer, which consists of two subunits: A long N-terminal fragment and short C-terminal fragment. Its cytoplasmic tail takes part in intracellular signaling by interfering with different proteins and affecting their function (4). The cytoplasmic tail of MUC1 interacts with different molecules, which are also overexpressed in cancer, such as ER, β-catenin and ErbB growth factor receptor tyrosine kinases (7).

Our recent study synthesized and evaluated the anticancer potential of novel diisoquinoline derivatives in breast and gastric cancer cells (8). The novel compounds were involved in the inhibition of AKT and ERK1/ERK2 (8). It was also demonstrated that the new diisoquinoline derivatives could modulate both apoptotic pathways. Another previous study demonstrated that all novel synthesized compounds activated the initiator and executioner caspases, such as caspase-8,

caspase-9, caspase-10 and caspase-3, compared with untreated breast cancer cells (9).

The aim of the present study was to examine the multi-targeted potential of a monoclonal antibody against MUC1 and novel octahydropyrazin[2,1-a:5,4-a']diisoquinoline derivative (OM-86II) in ER-positive MCF-7 human breast cancer cells. The results of the present study were compared with the findings concerning etoposide used together with anti-MUC1 antibody as well as with monotherapy. Etoposide is a widely used drug for chemotherapy and its molecular mechanism of action is associated with the inhibition of topoisomerase II (10).

Materials and methods

Materials. Stock cultures of human MCF-7 breast cancer cells were purchased from The American Type Culture Collection. DMEM and FBS used in cell culture were products of Gibco; Thermo Fisher Scientific, Inc. Glutamine, penicillin and streptomycin were obtained from Quality Biological, Inc. The JC-1 MitoScreen kit was supplied by BD Pharmigen; BD Biosciences. ELISA kits used to detect the concentrations of matrix metalloproteinase (MMP)-2, MMP-9, tumor necrosis factor (TNF)-α, cyclooxygenase (COX)-2, mTOR and soluble intercellular adhesion molecule (sICAM)1 were obtained from Wuhan EIAab Science Co., Ltd. (cat. nos. E0100 h, E0553 h, E0133 h, E0699 h, E14969 h and EH0161). Etoposide was obtained from Sigma-Aldrich; Merck KGaA and the purity of the compound was >98%. Monoclonal anti-MUC1 antibody (cat. no. MA1-06503) was a product of Thermo Fisher Scientific, Inc.

Nuclear magnetic resonance (NMR) spectra were recorded using a Varian VNMR500 spectrometer (Varian, Inc.). Chemical shifts are quoted in parts per million relative to TMS for ^{1}H and toluene-d_8 for ^{13}C NMR. Coupling constants *J* are reported in Hz. Mass spectra were recorded using an AMD-604 Intectra GmbH mass spectrometer (Waters Corporation).

Compounds. OM-86II was synthesized using previously standardized methods (9,11). The synthesis and physicochemical characterization of a compound 15a was presented in our previous study (11). Compound 15a (0.3 mmol; 169 mg) was dissolved in acetonitrile (15 ml) and cooled to 0˚C. Into intensively stirred reaction mixture, a water solution (10 ml) of cerium ammonium nitrate (1 mmol; 326 mg) was added dropwise. Stirring was continued at room temperature until the reaction was over (~2 h), poured into cold sodium dithionate (60 ml; 1M), extracted with dichloromethane (3x40 ml), dried with magnesium sulphate, filtrated and concentrated. The crude product was purified on silica gel using gradient DCM/MeOH (1-10% MeOH) as an eluent (Fig. 1).

Yield: 79 mg, 45%. Semisolid. ^{1}H NMR (toluene-d_8, 80˚C, 500 MHz): 7.84 - 7.80 (m, 2H), 7.66 - 7.1 (m, 2H), 7.17 - 7.11 (m, 3H), 7.11 - 7.00 (m, 3H), 6.80 (s, 1H), 6.78 (s, 1H), 6.54 (s, 1H), 6.37 (s, 1H), 3.85 (d, J=5.6 Hz, 1H), 3.70 (d, J=9.6 Hz, 1H), 3.56 (d, J=5.6 Hz, 1H), 3.46 (s, 3H), 3.44 (s, 3H), 3.37 (s, 3H), 3.26 - 3.21 (m, 4H), 3.10 - 2.91 (m, 2H), 2.90 - 2.71 (m, 3H), 2.58 - 2.50 (m, 2H). ^{13}C NMR (toluene-d_8, 80˚C, 125 MHz): δ (ppm): 196.3, 151.5, 148.4, 148.3, 147.8, 147.0, 139.1, 134.1, 132.2, 132.0, 130.4, 130.1, 128.0, 128.0 127.7, 127.2, 126.3, 114.3, 113.7, 112.4, 111.9, 75.3, 69.0, 65.0, 57.0, 55.4, 55.1, 55.1, 55.1, 45.0, 32.9, 26.4. MS (ES, HR) m/z: (M+) calcd for $C_{36}H_{36}N_2O_5$: 576.6930; Found: 576.2626. Anal. Calcd for $C_{36}H_{36}N_2O_5$: C, 74.98; H, 6.29; N, 4.86; Found: C, 75.00; H, 6.20; N, 4.81.

Cell culture of MCF-7 cells. ER-positive breast cancer MCF-7 cells were maintained in DMEM supplemented with 10% FBS, 2 mM glutamine, 50 U/ml penicillin, 50 mg/ml streptomycin at 37˚C in a humidified atmosphere containing 5% CO_2. Sub-confluent cells were treated with 0.05% trypsin and 0.02% EDTA in calcium-free PBS, counted using a hemocytometer and seeded in 6-well plates (Nunc) in 2 ml growth medium (DMEM without phenol red with 10% CPSR1). The cells that reached ~80% confluency were used for the assays.

Treatment groups and conditions. MCF-7 breast cancer cells were incubated with anti-MUC1 (10 μg/ml), OM-86II (30 μM), OM-86II + anti-MUC1 (30 μM + 10 μg/ml), etoposide (30 μM) and etoposide + anti-MUC1 (30 μM + 10 μg/ml) for 24 and 48 h at 37˚C in 5% CO_2 in an incubator.

Cell viability assay. To examine the effect of the compounds on cell growth, MCF-7 cells were seeded in 6-well plates ($2x10^6$) and cultured as described. Cell cultures were incubated with varying concentrations of the compounds tested for 24 and 48 h. Then cells were washed three times with PBS and then incubated for 4 h in 1 ml MTT solution (0.5 mg/ml PBS) at 37˚C in 5% CO_2 in an incubator. The medium was removed and 1 ml 0.1 mol/l HCl in absolute isopropanol was added to the attached cells. The absorbance of the converted dye in living cells was measured at a wavelength of 570 nm (12).

[^{3}H]thymidine incorporation assay. To examine the effect of the compounds on cell proliferation, MCF-7 cells were seeded ($2x10^6$) in 6-well plates and cultured as described. Cell cultures were incubated with varying concentrations of the tested compounds and 0.5 μCi [^{3}H]thymidine for 24 h at 37˚C. The cells were harvested by trypsinization and washed several times in cold PBS (10 min/1.500 g) until the dpm in the washes were similar to the reagent control. Radioactivity was determined by liquid scintillation counting. [^{3}H]thymidine uptake is expressed as dpm/well (9).

Cell cycle analysis. The distribution of the cell cycle phases was analyzed by flow cytometry. Briefly, MCF-7 breast cancer cells were seeded into 6-well plates at a density of $2.5x10^5$ cells/well and treated with the compounds for 24 and 48 h. After incubation, the cells were harvested and then fixed with 1 ml 70 % ethanol and kept overnight at -20˚C. Before analysis, the cells were resuspended in PBS, treated with 50 μg/ml DNase-free RNase A solution (Promega Corporation), and stained for 30 min at 37˚C with 100 μg/ml propidium iodide (PI; ImmunoChemistry Technologies, LLC; cat. no. 638). The FACSCanto II flow cytometer (BD Biosciences) was used to read the fluorescence and the results were analyzed using FACSDiva software (version 6.1.3; BD Biosciences Systems) (13).

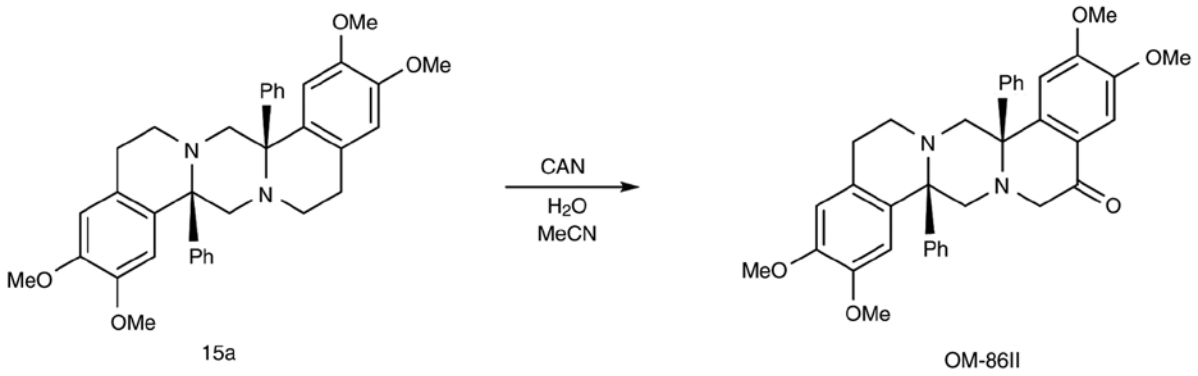

Figure 1. Synthesis of (8aS,16aS)-2,3,10,11-tetramethoxy-8a,16a-diphenyl-8,8a,13,14,16,16a-hexahydropyrazino[2,1-a:5,4-a']diisoquinolin-5(6H)-one. CAN, cerium ammonium nitrate; OM-86II, octahydropyrazin[2,1-a:5,4-a']diisoquinoline derivative.

Determination of mitochondrial membrane potential. Disruption of the mitochondrial membrane potential was assessed using the lipophilic cationic probe 5,5',6,6'-tetrachloro-1,1',3,3'-tetraethylbenzimidazolcarbocyanine iodide (JC-1 Mitoscreen kit; BD Biosciences) as previously described (14). Briefly, unfixed cells were washed and resuspended in PBS supplemented with JC-1. The cells were then incubated for 15 min. at room temperature in the dark, washed and resuspended in PBS for immediate flow cytometry analysis using a FACSCanto II flow cyometer. The percentage of cells with disrupted MMP was calculated using FACSDiva software (version 6.1.3; BD Biosciences).

Dual acridine orange/ethidium bromide fluorescent staining. To confirm that the compounds induce apoptosis, dual acridine orange/ethidium bromide fluorescent staining was assessed and visualized under a fluorescent microscope (Nikon Eclipse Ti; Nikon Corporation). MCF-7 breast cancer cells were treated with the compounds for 24 and 48 h. The cell suspension (250 μl) was stained for 10 min at room temperature in the dark with 10 μl dye mixture (10 μM acridine orange and 10 μM ethidium bromide), which was prepared in PBS. Cells cultured in a drug-free medium were used as controls. The morphology of two hundred cells per sample was examined by fluorescent microscopy (magnification, x100) within 20 min. The results were analyzed with NIS-Elements software (version 3.10; Nikon Corporation).

Flow cytometry assessment of Annexin V binding. The effect of the compounds on the induction of apoptosis after 24 and 48 h of incubation was assessed using a Becton Dickinson FACSCanto II flow cytometer (BD Biosciences). The assessment allows checking the loss of asymmetry of phospholipids on the cell membrane. Cells were trypsinized, resuspended in DMEM and then in binding buffer. Next, they were stained with FITC Annexin V and PI for 15 min at room temperature in the dark, according to the manufacturer's protocol (FITC Annexin V Apoptosis Detection kit II; BD Biosciences). Cells cultured in a drug-free medium were used as controls. The optimal parameter settings were found using a positive control (cells incubated with 3% formaldehyde in buffer during 30 min on ice). Forward scatter and side scatter signals were detected on a logarithmic scale histogram. FITC was detected in the FL1 channel (FL1 539; Threshold-value 52). The results were analyzed with FACSDiva software (version 6.1.3; BD Biosciences).

Determination of matrix metalloproteinase (MMP)-2, MMP-9, tumor necrosis factor (TNF)-α, cyclooxygenase (COX)-2, mTOR and soluble intercellular adhesion molecule (sICAM)1. High sensitivity assay ELISA kits (Wuhan EIAab Science Co., Ltd.) were used to determine the concentrations of proteins in supernatants from cell culture or in cell lysates (15) after 24 and 48 h of incubation with the compounds. There was no cross-reactivity or interference by other proteins present in biological samples. The microtiter plate provided in this kit was pre-coated with an antigen-specific antibody. Standards and samples were added to the appropriate microtiter plate wells. After 2 h of incubation at 37˚C, the plate was incubated with biotin-conjugated antibody from the kits for 1 h at 37˚C. Then, the microplate wells were aspirated and washed three times, and then incubated for 1 h at 37˚C with avidin conjugated to horseradish peroxidase. Then, a 3,3',5,5'-tetramethylbenzidine substrate solution was added to each well. The enzyme-substrate reaction was terminated by the addition of a sulfuric acid solution and the color change was measured spectrophotometrically at a wavelength of 450±2 nm. The concentration of antigen in the samples was determined by comparing the optical density of the samples to the standard curve.

Statistical analysis. All numerical data are presented as the mean ± SD from three independent experiments. The statistical analysis was performed using GraphPad Prism Version 6.0 (GraphPad Software, Inc.). All datasets were analyzed using ANOVA and Tukey's test. $P<0.05$ was considered to indicate a statistically significant difference.

Results

Novel OM-86II combined with anti-MUC1 antibody decreases cell viability and proliferation of MCF-7 breast cancer cells. The effects of etoposide, a novel diisoquinoline derivative (OM-86II) and an anti-MUC1 antibody as well as etoposide or OM-86II in combination with anti-MUC1 antibody on cell viability and DNA biosynthesis in MCF-7 breast cancer cells were examined (Figs. 2 and 3). The cell viability was analyzed after 24 and 48 h

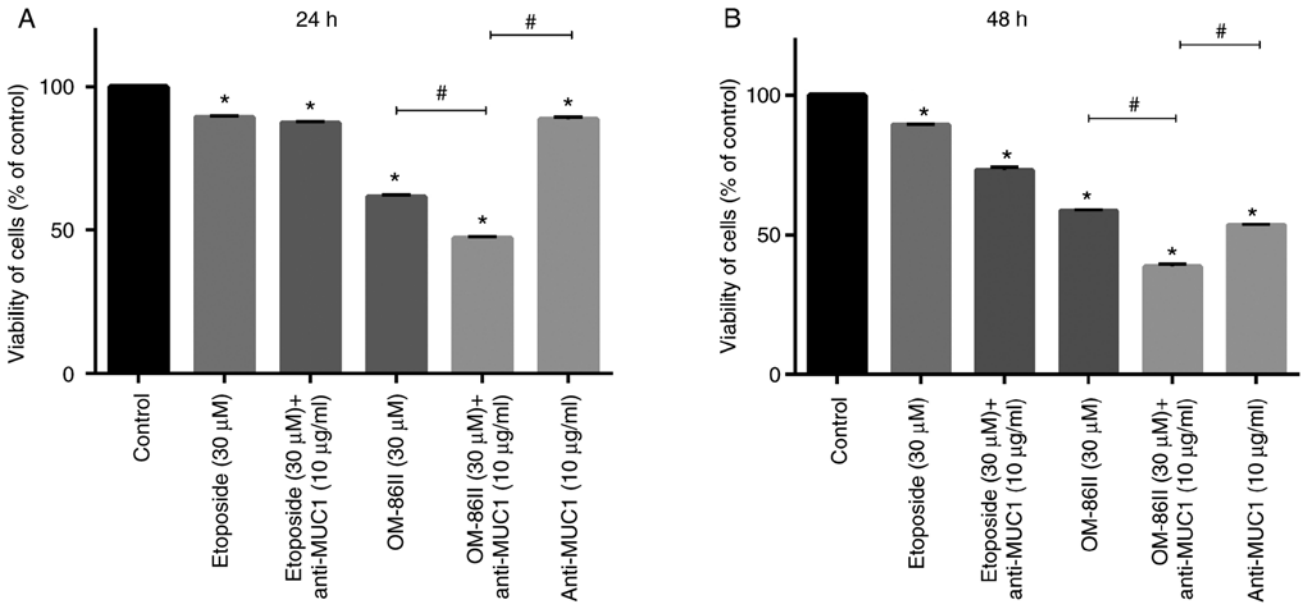

Figure 2. Novel OM-86II combined with anti-MUC1 antibody decreases cell viability of MCF-7 breast cancer cells. Viability of MCF-7 breast cancer cells treated for (A) 24 and (B) 48 h with anti-MUC1 (10 μg/ml), OM-86II (30 μM), OM-86II + anti-MUC1 (30 μM + 10 μg/ml), etoposide (30 μM) and etoposide + anti-MUC1 (30 μM + 10 μg/ml). The data are presented as the mean ± SD from three independent experiments (n=3) conducted in duplicate. *P<0.05 vs. control group; #P<0.05. MUC1, mucin-1; OM-86II, octahydropyrazin[2,1-a:5,4-a']diisoquinoline derivative.

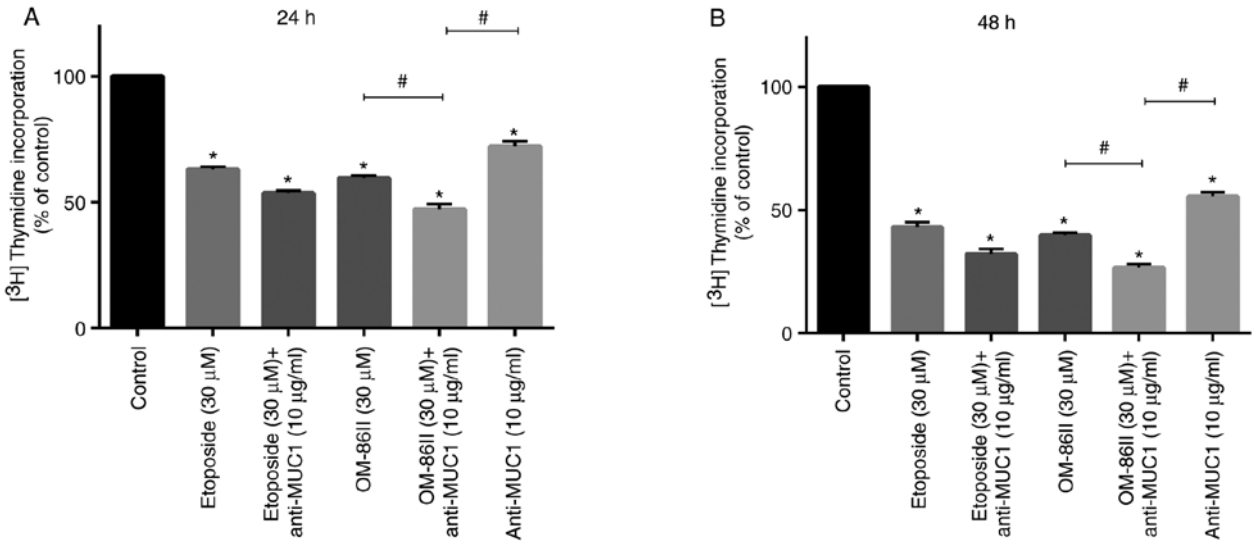

Figure 3. Novel OM-86II combined with anti-MUC1 antibody decreases proliferation of MCF-7 breast cancer cells. Antiproliferative effects of anti-MUC1 (10 μg/ml), OM-86II (30 μM), OM-86II + anti-MUC1 (30 μM + 10 μg/ml), etoposide (30 μM), etoposide + anti-MUC1 (30 μM + 10 μg/ml) in cultured MCF-7 cells after (A) 24 and (B) 48-h incubation as measured by inhibition of [^{3}H]-thymidine incorporation into DNA. Data are presented as the mean ± SD from three independent experiments (n=3) conducted in duplicate. *P<0.05 vs. control group; #P<0.05. MUC1, mucin-1; OM-86II, octahydropyrazin[2,1-a:5,4-a'] diisoquinoline derivative.

of incubation with the agents tested. It was detected that the anti-MUC1 antibody used together with OM-86II represented the strongest cytotoxic and antiproliferative potential (Figs. 2 and 3). Such a combination decreased the number of viable cells to 47.1 and 38.8% after 24 and 48 h of incubation, respectively (Fig. 2). The combination of etoposide and anti-MUC1 antibody reduced the number of live cells to 87.4 and 73.2% after 24 and 48 h of incubation, respectively (Fig. 2). Monotherapy was not so efficient in decreasing the viability of MCF-7 cells. However, the most cytotoxic properties for monotherapy were observed after incubation with anti-MUC1 antibody, which reduced the viability of breast cancer cells to 53.4% after 48 h of incubation, respectively (Fig. 2).

The antiproliferative potential of the compounds tested was demonstrated by the incorporation of [^{3}H]-thymidine into the DNA of MCF-7 cells (Fig. 3). The combination of novel OM-86II with anti-MUC1 represented the strongest antiproliferative activity in MCF-7 breast cancer cells. We detected that such a combination inhibited DNA biosynthesis to 47.15 and 26.5% after 24 and 48 h of incubation, while etoposide with anti-MUC1 reduced [^{3}H]-thymidine incorporation to 53.64 and 32.12% after 24 and 48 h of incubation. Monotherapy

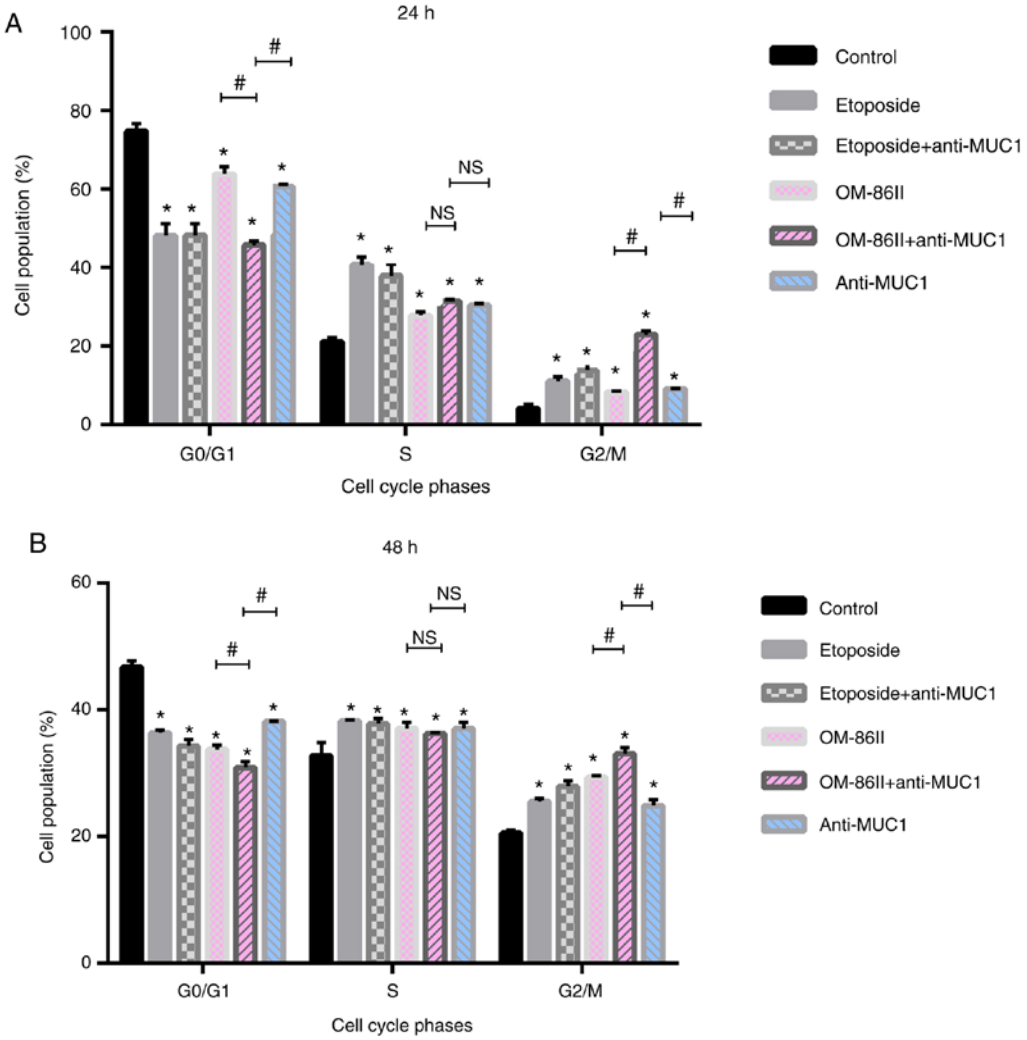

Figure 4. Novel OM-86II combined with anti-MUC1 antibody induces G_2/M cell cycle arrest in MCF-7 cells. Effect of anti-MUC1 (10 μg/ml), OM-86II (30 μM), OM-86II + anti-MUC1 (30 μM + 10 μg/ml), etoposide (30 μM) and etoposide + anti-MUC1 (30 μM + 10 μg/ml) on cell cycle distribution in human MCF-7 cells after (A) 24 and (B) 48 h of incubation. Data are presented as the mean ± SD from three independent experiments (n=3) conducted in duplicate. *P<0.05 vs. control group; #P<0.05. MUC1, mucin-1; OM-86II, octahydropyrazin[2,1-a:5,4-a']diisoquinoline derivative; ns, not significant.

was not so efficient, and in this case the most antiproliferative potential was demonstrated after incubation with OM-86II, which inhibited the [^{3}H]-thymidine incorporation into DNA of breast cancer cells to 59.6 and 39.8% after 24 and 48 h of incubation (Fig. 3).

Novel OM-86II combined with anti-MUC1 antibody induces G_2/M cell cycle arrest in MCF-7 cells. Anticancer agents can be designed to target specific cell cycle checkpoints in cancer cells and are able to induce cell death (16). Cell cycle analysis revealed that monotherapy as well as a combination of compounds (OM-86II, etoposide), together with anti-MUC1 antibody, induced G_2/M arrest in MCF-7 breast cancer cells. As shown in Fig. 4A, the percentage of cells in the G_2/M phase increased from 4.1% in the untreated control to 22.1% after treatment with OM-86II and anti-MUC1 (30 μM + 10 μg/ml), 13.6% after treatment with etoposide and anti-MUC1 (30 μM + 10 μg/ml), 8.3% after treatment with OM-86II (30 μM), 11% after treatment with etoposide (30 μM) and 9% after treatment with anti-MUC1 antibody (10 μg/ml). Upon prolongation of the exposure time to 48 h, the highest percentages of cells were arrested in the G_2/M phase after treatment with OM-86II combined with anti-MUC1 antibody (33.0%; Fig. 4B).

Novel OM-86II combined with anti-MUC1 antibody induces apoptosis and decreases mitochondrial membrane potential in breast cancer cells. Dual acridine orange/ethidium bromide fluorescent staining was performed to visualize viable, apoptotic and necrotic cells after treatment with the compounds used alone and in combination with anti-MUC1 antibody (Fig. 5). Control (untreated) cells were displayed as green fluorescence. Bright green fluorescence was characteristic of early apoptotic cells, whereas an orange color was specific to late apoptotic cells. The present study demonstrated that the combination of OM-86II and anti-MUC1, resulted in the highest number of apoptotic cells. Bright green fluoresence as well as orange fluorescence was observed. The strongest pro-apoptotic effect was observed after 48 h of incubation (Fig. 5B).

An Annexin V binding assay was performed to confirm the results obtained by fluorescence microscopy. The results are presented in Fig. 6. The histograms showed viable, early and

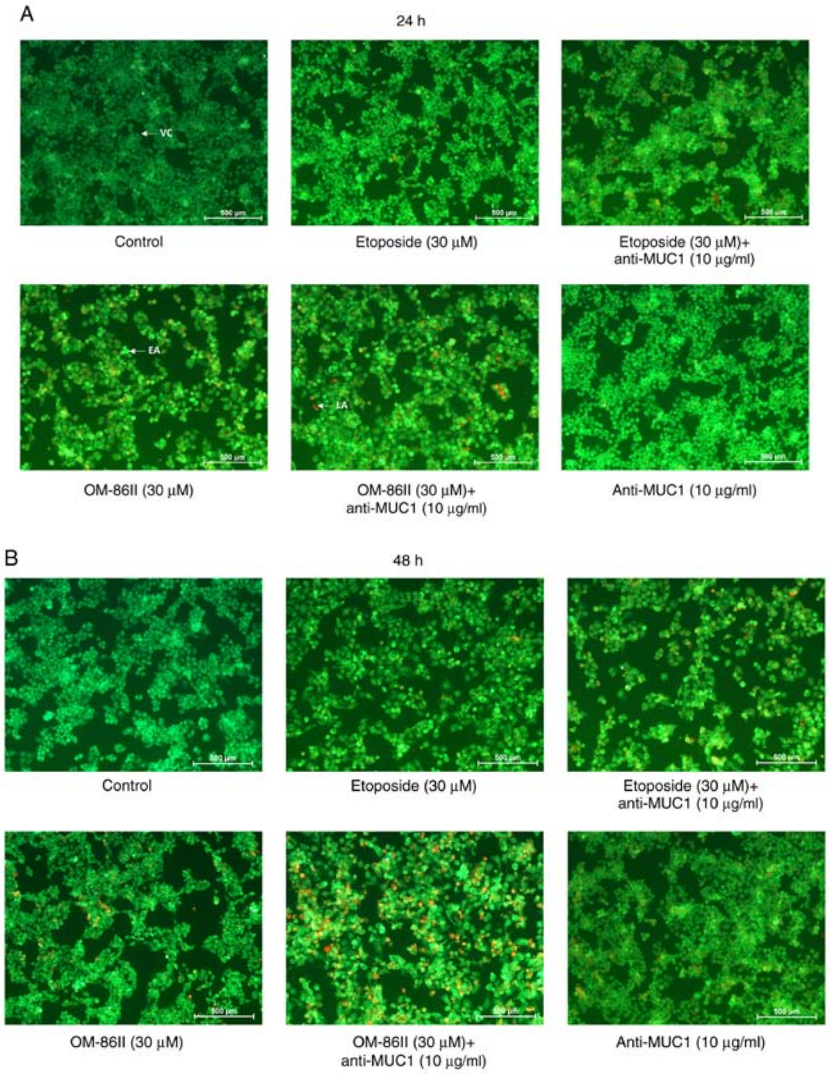

Figure 5. Novel OM-86II combined with anti-MUC1 antibody induces apoptosis in MCF-7 breast cancer cells. Induction of apoptosis in human MCF-7 cells treated for (A) 24 and (B) 48 h with anti-MUC1 (10 μg/ml), OM-86II (30 μM), OM-86II + anti-MUC1 (30 μM + 10 μg/ml), etoposide (30 μM) and etoposide + anti-MUC1 (30 μM + 10 μg/ml) evaluated by fluorescent microscopy after acridine orange and ethidium bromide staining. Magnification, x100. MUC1, mucin-1; OM-86II, octahydropyrazin[2,1-a:5,4-a']diisoquinoline derivative; VC, viable cells; EA, early apoptosis; LA, late apoptosis.

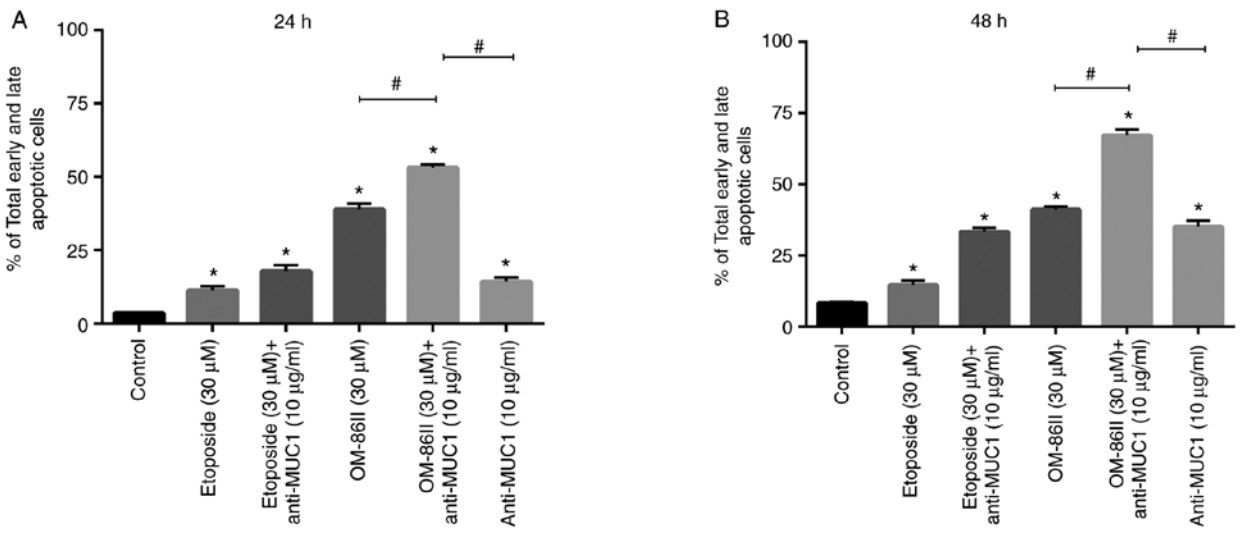

Figure 6. Novel OM-86II combined with anti-MUC1 antibody induces programmed cell death in MCF-7 breast cancer cells. Induction of apoptosis in human MCF-7 cells treated for (A) 24 and (B) 48 h with anti-MUC1 (10 μg/ml), OM-86II (30 μM), OM-86II + anti-MUC1 (30 μM + 10 μg/ml), etoposide (30 μM) and etoposide + anti-MUC1 (30 μM + 10 μg/ml) evaluated by flow cytometry. Data are presented as the mean percentage values from three independent experiments (n=3) conducted in duplicate. *P<0.05 vs. control group; $^{\#}$P<0.05. MUC1, mucin-1; OM-86II, octahydropyrazin[2,1-a:5,4-a']diisoquinoline derivative.

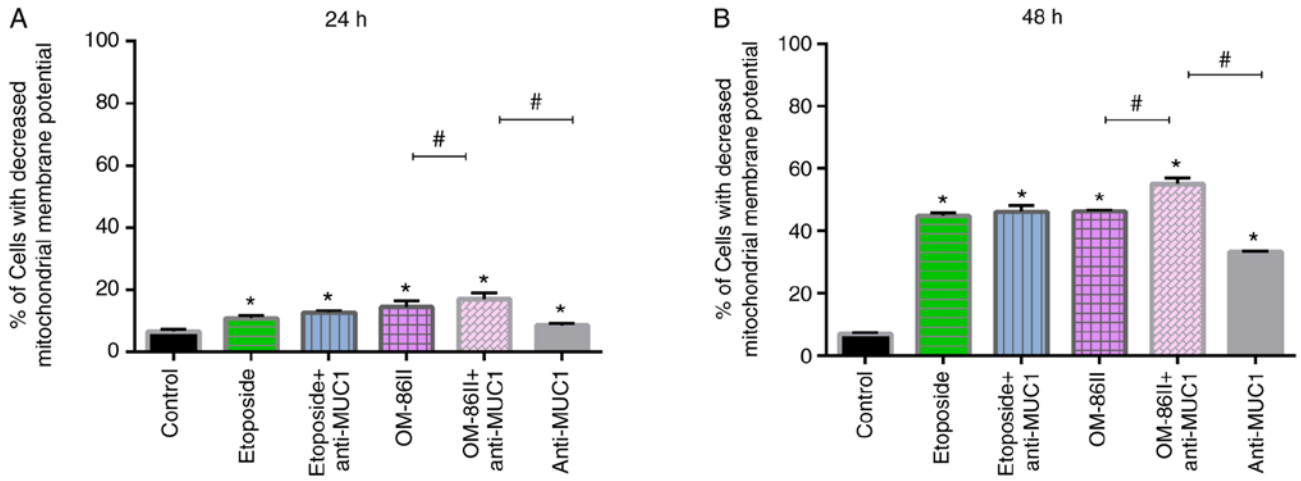

Figure 7. Novel OM-86II combined with anti-MUC1 antibody decreases mitochondrial membrane potential in breast cancer cells. Loss of mitochondrial membrane potential in MCF-7 breast cancer cells treated for (A) 24 and (B) 48 h with anti-MUC1 (10 μg/ml), OM-86II (30 μM), OM-86II + anti-MUC1 (30 μM + 10 μg/ml), etoposide (30 μM) and etoposide + anti-MUC1 (30 μM + 10 μg/ml) as measured by JC-1 fluorescence. Data are presented as the mean percentage values from three independent experiments (n=3) conducted in duplicate. *P<0.05 vs. control group; $^{\#}$P<0.05. MUC1, mucin-1; OM-86II, octahydropyrazin[2,1-a:5,4-a']diisoquinoline derivative.

late apoptotic cells, and necrotic cells. In total, 11.3% apoptotic cells after treatment with etoposide and 17.9% with combination of etoposide and anti-MUC1 were observed after 24-h incubation. OM-86II demonstrated stronger pro-apoptotic potential and 38.9% of early and late apoptotic cells were detected. The most significant effect was observed after 24-h incubation with anti-MUC1 and OM-86II. In that case, 53.1% of apoptotic cells were detected (Fig. 6A). After the next 24 h of incubation, the pro-apoptotic effect was enhanced after all treatments, but the percentage of apoptotic cells (67.1%) was the highest after 48 h of incubation with anti-MUC1 and OM-86II (Fig. 6B).

The mitochondrial membrane potential of the cells was detected after 24 and 48 h of incubation (Fig. 7). It was identified that all the compounds significantly decreased the mitochondrial membrane potential compared with the control after 48 h of incubation (Fig. 7B). In the control MCF-7 cells, 7.4% of cells with reduced mitochondrial membrane potential were detected. After 48 h of incubation with etoposide and etoposide with anti-MUC1, 44.9 and 46.2% of cells, respectively, with reduced mitochondrial membrane potential were detected. The compound OM-86II led to a higher percentage of cells with decreased mitochondrial membrane potential (46.4%) as compared with etoposide and anti-MUC antibody. The combination of OM-86II with anti-MUC1 antibody reduced the mitochondrial membrane potential the most; it was observed that 55% of cells had reduced mitochondrial membrane potential (Fig. 7B).

Novel OM-86II combined with anti-MUC1 antibody decreases the concentration of MMP-2 and MMP-9 in supernatants from MCF-7 cell cultures. ELISA, a quantitative method, was chosen instead of western blotting to measure the concentration of analyzed proteins. The concentration of MMP-2 was detected after 24 and 48 h of incubation with etoposide, etoposide with anti-MUC1, OM-86II, OM-86II with anti-MUC1 and anti-MUC1 antibody (Fig. 8). It was identified that OM-86II with anti-MUC1 antibody decreased the concentration of MMP-2 in supernatants from the cell cultures (1.5 ng/ml) the most in comparison with control, where the concentration of MMP-2 was 1.8 ng/ml (Fig. 8B).

The concentration of MMP-9 was additionally detected (Fig. 9). The most significant change in the concentration of MMP-9 was observed after 48 h of incubation with the compounds tested (Fig. 9B). The concentration of MMP-9 in the control sample after 48 h was 24 ng/ml. It was demonstrated that novel OM-86II reduced the concentration of MMP-9 to 16 ng/ml and the combination of OM-86II with anti-MUC1 antibody reduced the concentration to 13 ng/ml. Etoposide alone and in combination with anti-MUC1 antibody significantly increased the concentration of MMP-9 to 48 ng/ml.

Novel OM-86II combined with anti-MUC1 antibody decreases the concentration of TNF-α and COX-2. The prolonged exposition of epithelial cells to different factors and activation of inflammatory pathways are associated with tumorigenesis (17). Several previous studies have demonstrated an anticancer effect after the inhibition of TNF-α and its receptors; such an effect was observed in animal models of breast cancer (18-25). In the present study, the concentration of TNF-α was detected after 24 and 48 h of incubation with the different treatments (Fig. 10). The most significant changes in TNF-α concentration were detected after 48 h of incubation with the compounds tested (Fig. 10B). The strongest inhibition of TNF-α release was observed after combined treatment with OM-86II and anti-MUC1 antibody. The concentration of TNF-α was 15 pg/ml, as compared with 19.5 pg/ml in the control sample.

Cancer cells with overexpressed COX-2 are resistant to apoptosis, and COX-2 acts as a key driver in increased growth and invasion of cancer cells via different molecular signaling pathways (17). The present study demonstrated that the combination therapy based on OM-86II and anti-MUC1 antibody led to decreased concentration of COX-2 in cell lysates in comparison with the control (Fig. 11). Etoposide and anti-MUC1 as well as OM-86II and anti-MUC1 decreased

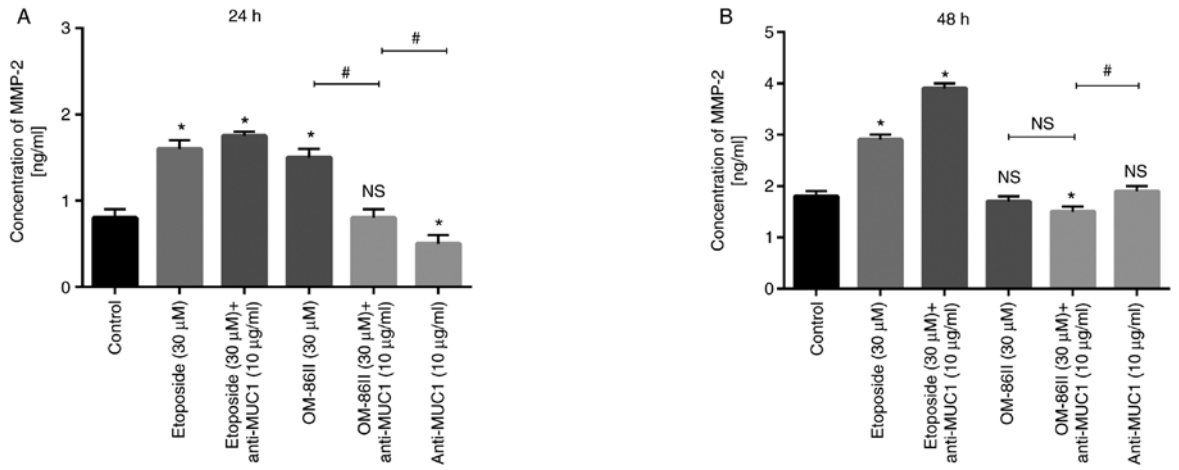

Figure 8. Novel OM-86II combined with anti-MUC1 antibody decreases the concentration of MMP-2 in supernatants from MCF-7 cell cultures. Concentration of MMP-2 in breast cancer MCF-7 cells after (A) 24 h and (B) 48-h incubation with anti-MUC1 (10 μg/ml), OM-86II (30 μM), OM-86II + anti-MUC1 (30 μM + 10 μg/ml), etoposide (30 μM) and etoposide + anti-MUC1 (30 μM + 10 μg/ml). Data are presented in ng/ml. *P<0.05 vs. control group; #P<0.05. MMP-2, matrix metalloproteinase-2; MUC1, mucin-1; OM-86II, octahydropyrazin[2,1-a:5,4-a']diisoquinoline derivative; ns, not significant.

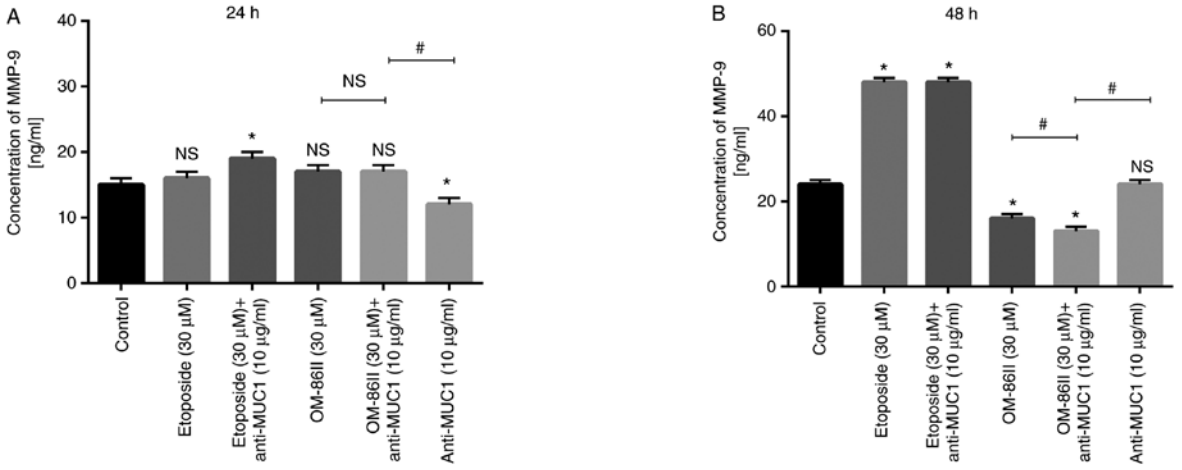

Figure 9. Novel OM-86II combined with anti-MUC1 antibody decreases the concentration of MMP-9 in supernatants from MCF-7 cell cultures. Concentration of MMP-9 in breast cancer MCF-7 cells after (A) 24 and (B) 48-h incubation with anti-MUC1 (10 μg/ml), OM-86II (30 μM), OM-86II + anti-MUC1 (30 μM + 10 μg/ml), etoposide (30 μM) and etoposide + anti-MUC1 (30 μM + 10 μg/ml). Data are presented in ng/ml. *P<0.05 vs. control group; #P<0.05. MMP-9, matrix metalloproteinase; MUC1, mucin-1; OM-86II, octahydropyrazin[2,1-a:5,4-a']diisoquinoline derivative; ns, not significant.

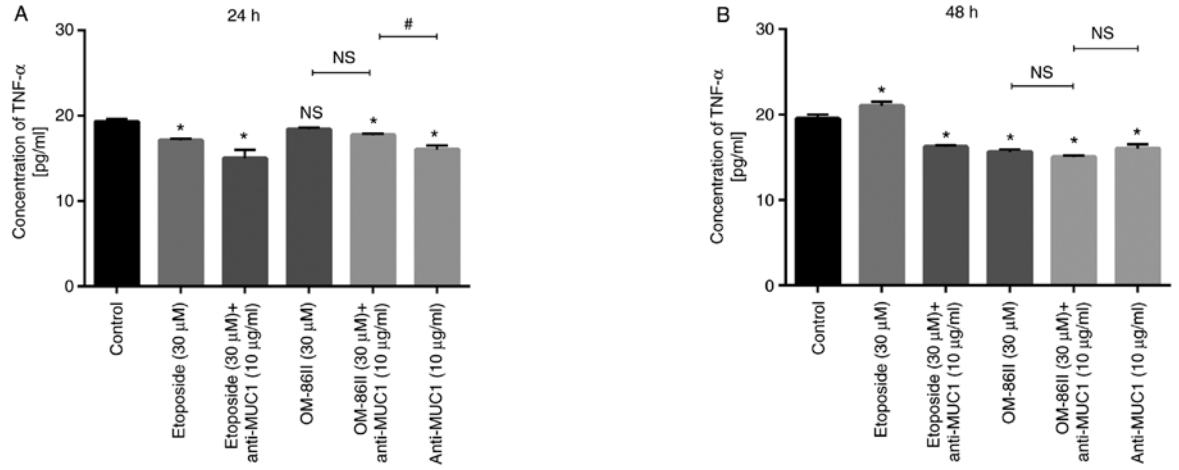

Figure 10. Novel OM-86II combined with anti-MUC1 antibody decreases the concentration of TNF-α. Concentration of TNF-α in breast cancer MCF-7 cells after (A) 24 h and (B) 48-h incubation with anti-MUC1 (10 μg/ml), OM-86II (30 μM), OM-86II + anti-MUC1 (30 μM + 10 μg/ml), etoposide (30 μM) and etoposide + anti-MUC1 (30 μM + 10 μg/ml). Data are presented in pg/ml. *P<0.05 vs. control group; #P<0.05. TNF-α, tumor necrosis factor-α; MUC1, mucin-1; OM-86II, octahydropyrazin[2,1-a:5,4-a']diisoquinoline derivative; ns, not significant.

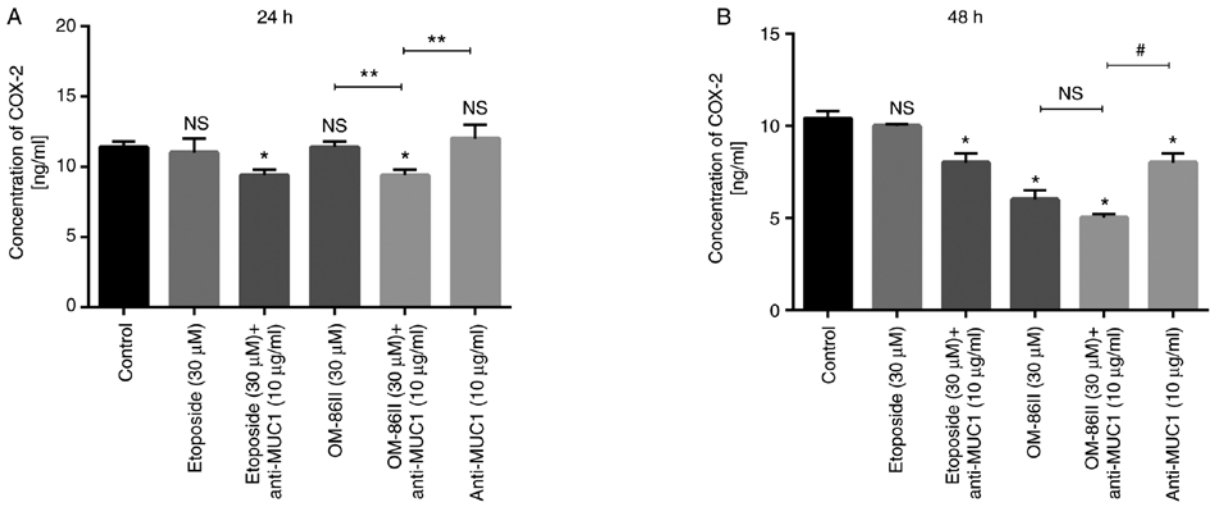

Figure 11. Novel OM-86II combined with anti-MUC1 antibody decreases the concentration of COX-2. Concentration of COX-2 in breast cancer MCF-7 cells after (A) 24 and (B) 48-h incubation with anti-MUC1 (10 μg/ml), OM-86II (30 μM), OM-86II + anti-MUC1 (30 μM + 10 μg/ml), etoposide (30 μM) and etoposide + anti-MUC1 (30 μM + 10 μg/ml). Data are presented in ng/ml. *P<0.05 vs. control group; #P<0.05. COX-2, cyclooxygenase-2; MUC1, mucin-1; OM-86II, octahydropyrazin[2,1-a:5,4-a']diisoquinoline derivative; ns, not significant.

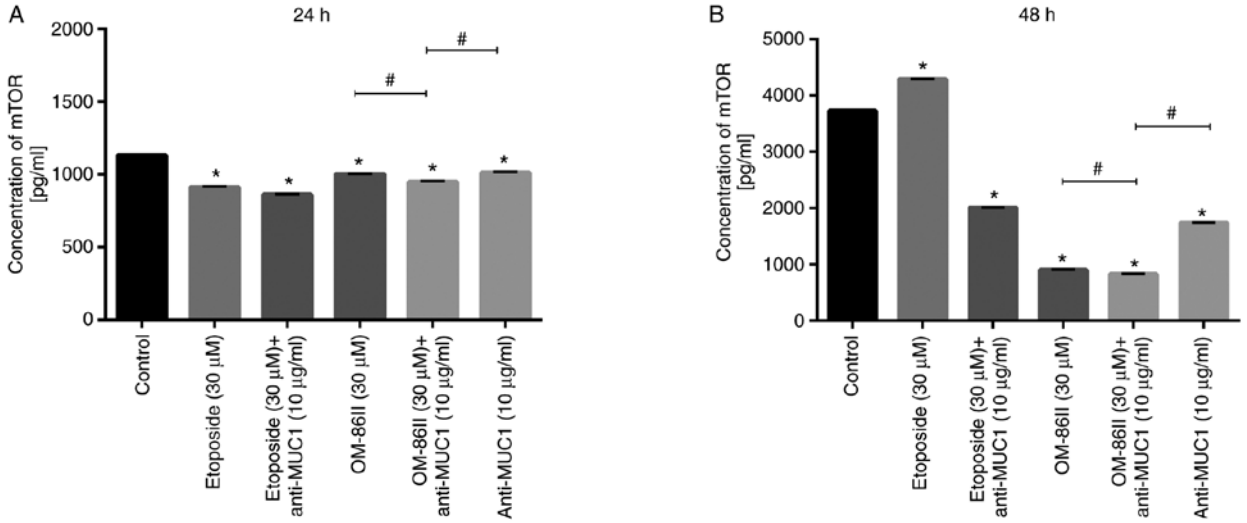

Figure 12. Novel OM-86II combined with anti-MUC1 antibody decreases the concentration of mTOR. Concentration of mTOR in breast cancer MCF-7 cells after (A) 24 and (B) 48-h incubation with anti-MUC1 (10 μg/ml), OM-86II (30 μM), OM-86II + anti-MUC1 (30 μM + 10 μg/ml), etoposide (30 μM) and etoposide + anti-MUC1 (30 μM + 10 μg/ml). Data presented in ng/ml. *P<0.05 vs. control group; #P<0.05. MUC1, mucin-1; OM-86II, octahydropyrazin[2,1-a:5,4-a'] diisoquinoline derivative.

the concentration of COX-2 to 9.4 ng/ml after 24-h incubation compared with the control, where the concentration of COX-2 was 11.4 ng/ml (Fig. 11A). After 48 h of incubation, both analyzed combinations of the compounds (etoposide and anti-MUC1, and OM-86II and anti-MUC1) significantly decreased the COX-2 level. However, the strongest effect was observed after treatment with OM-86II and the anti-MUC1 antibody; 5 ng/ml of COX-2 was detected in the cell lysates. The concentration of COX-2 after treatment with etoposide and anti-MUC1 was 8 ng/ml and the difference was also statistically significant in comparison with the control (P<0.05; Fig. 11B).

Novel OM-86II combined with anti-MUC1 antibody decreases the concentration of mTOR. The activated PI3K/Akt/mTOR signaling pathway is responsible for tumor growth and cancer progression (26,27). Several agents targeted to one or more components of the PI3K/AKT/mTOR pathway were examined for the treatment of ER-positive breast cancer in clinical trials (28). The concentration of mTOR in cell lysates was determined after 24 and 48 h of incubation with the compounds tested (Fig. 12). Both monotherapy and combined therapy significantly decreased the concentration of mTOR in comparison with the untreated control after 24 h of incubation (P<0.05; Fig. 12A). The concentration of mTOR in the cell lysates was 949 pg/ml after treatment with OM-86II and anti-MUC1, while in the control sample the concentration was 1,131 pg/ml. The concentration of mTOR was 861 pg/ml after treatment with etoposide and anti-MUC1 antibody (Fig. 12A). After 48 h, it was observed that all the compounds tested

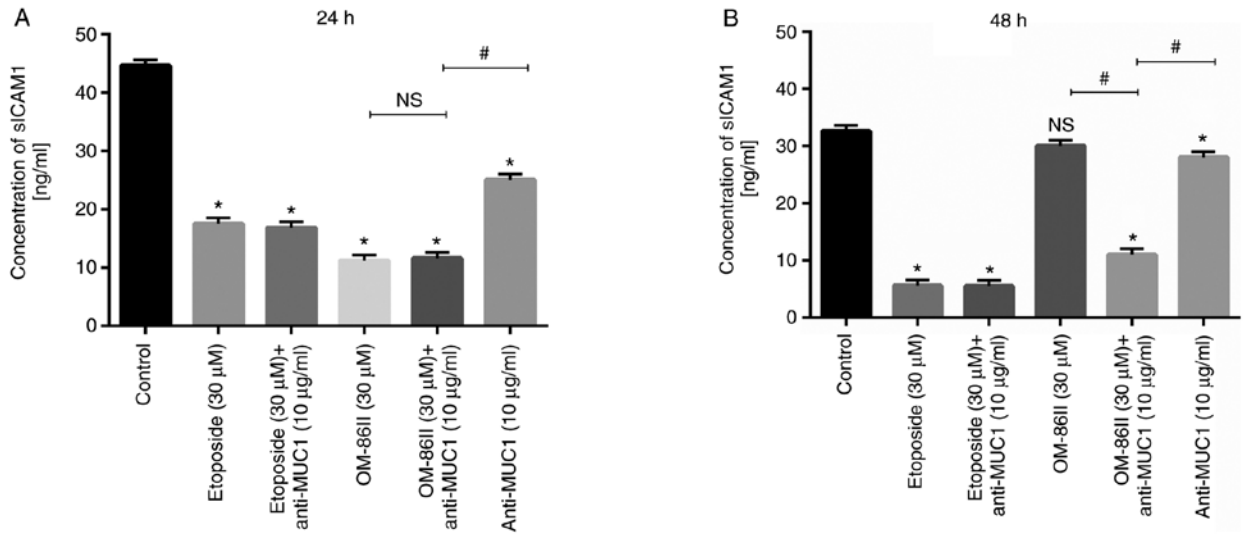

Figure 13. Novel OM-86II combined with anti-MUC1 antibody decreases the concentration of sICAM1. Concentration of sICAM1 in breast cancer MCF-7 cells after (A) 24 and (B) 48-h incubation with anti-MUC1 (10 μg/ml), OM-86II (30 μM), OM-86II+anti-MUC1 (30 μM + 10 μg/ml), etoposide (30 μM), etoposide + anti-MUC1 (30 μM + 10 μg/ml). Data are presented in ng/ml. *P<0.05 vs. control group; #P<0.05. sICAM1, soluble intercellular adhesion molecule 1; MUC1, mucin-1; OM-86II, octahydropyrazin[2,1-a:5,4-a']diisoquinoline derivative; ns, not significant.

except for etoposide significantly reduced the concentration of kinase. The lowest concentration of mTOR was detected after incubation with OM-86II and anti-MUC1 (826 pg/ml) compared with the control (3,729 pg/ml; Fig. 12B).

Novel OM-86II combined with anti-MUC1 antibody decreases the concentration of sICAM1. MUC1 interacts with ICAM-1 to facilitate the migration of tumor cells (29). The Src-CrkL-Rac1/Cdc42 signaling pathway plays the most significant role in promoting the migratory behavior of breast cancer cells, and upon ligation with sICAM-1 it connects with the MUC1 cytoplasmic domain and initiates cytoskeletal rearrangements (30). The present study demonstrated that all the tested compounds decreased sICAM1 concentration in supernatants from cell cultures (Fig. 13). The most significant change was observed after combined treatment. The concentration of sICAM1 after 24 and 48 h of incubation with etoposide and anti-MUC1 was 16.8 and 5.5 ng/ml, respectively. After 24 and 48 h of incubation OM-86II used together with anti-MUC1 significantly decreased the sICAM1 concentration to 11.6 and 11 ng/ml, respectively.

Discussion

Current evidence suggested that MUC1 is involved in growth, invasion, promotion of angiogenesis and chemoresistance to programmed cell death, induced by DNA damage, oxidative stress and hypoxia (31-35). Therapies targeting MUC1 include monoclonal antibodies, vaccines or small molecules (aptamers). However, none of them are currently used in clinical application and there is still a need to evaluate the most promising strategy in anticancer treatment based on MUC1 as a target (36). Combination of a monoclonal antibody with novel chemotherapeutic agents represents a more efficient approach in cancer treatment.

Disorders of cell cycle control and resistance to apoptosis represent the most characteristic features of cancer cells (37). The present study demonstrated that combined treatment based on an anti-MUC1 antibody with a novel diisoquinoline derivative (OM-86II) is an effective strategy in decreasing the number of viable cells and inhibiting the proliferation of MCF-7 breast cancer cells. The tested compounds led to the induction of apoptosis, decreased the mitochondrial membrane potential and induced a G_2/M cell cycle arrest in MCF-7 cells.

The extracellular matrix (ECM) plays an essential role in the regulation of different signaling pathways, such as PI3K/AKT, ERK and Src-FAK, and its function in tumor progression has also been demonstrated in many previous studies (38,39). MMPs are the enzymes responsible for degradation of ECM proteins and promotion of breast cancer progression (40). Metalloproteinases take part in the remodeling of the ECM in tumor invasion (41). A high serum MMP-2 level is associated with an adverse prognosis in node-positive breast carcinoma (42). MMP-9 plays a crucial role in cancer growth and invasion. Its overexpression was correlated with poor prognosis and worse patient survival (43). MMP-9 is also responsible for destruction of collagen type IV and other ECM components (44). It is known that both MMP-2 and MMP-9 are key players of breast cancer invasion and metastasis (45). The present study demonstrated that OM-86II with an anti-MUC1 antibody significantly decreased the level of the MMPs analyzed. The association between the process of chronic inflammation and tumor progression is still of interest; anti-inflammatory agents can be beneficial in cancer therapy. The expression of pro-inflammatory cytokine TNF-α was increased in 85% of breast tumors in patients, whereas it was only minimally expressed in normal breast epithelial cells (46). A previous study conducted by Hosseini *et al* (47) demonstrated that β-D mannuronic acid decreased the relative mRNA expression level of inflammatory chemokines and other factors responsible for tumor growth, such as vascular endothelial growth factor, MMP-2, MMP-9 and hypoxia-inducible factor-1α. In the present study, it was demonstrated that the combination of anti-MUC1 with OM-86II decreased the concentration of pro-inflammatory cytokine TNF-α in the cell culture media.

In a previous study where COX-2 expression was analyzed, it was identified that COX-2 was only expressed in tumors, and its expression was correlated with unfavorable prognosis (17). The effect of treatments on the concentration of COX-2 was studied in the present study and it was identified that anti-MUC1 used together with OM-86II significantly decreased the concentration after 24 and 48 h of incubation. Such a strategy was more efficient than monotherapy and the combination of anti-MUC1 with etoposide.

In MCF-7 breast cancer cells, the activated PI3K/AKT/mTOR signaling pathway (48) leads to increased cellular growth and survival (26,27). Therefore, the effect of the compounds tested on the concentration of mTOR was determined in MCF-7 cell lysates. After 48 h of incubation with the combination of anti-MUC1 and OM-86II, the highest decrease in mTOR concentration was observed compared with the other compounds. The inhibitory effect was also much stronger than the combination of anti-MUC1 and etoposide.

Some researchers have shown that breast cancer types, which exhibit increased expression of MUC1, are more likely to metastasize. MUC1 is able to induce the Src-CrkL-Rac1/Cdc42 signaling pathway upon ligation to the ICAM-1 (29,30). The activated pathway leads to increased migration of breast cancer cells (30). Rahn *et al* (49) showed that breast cancer cells with overexpressed MUC1 were able to migrate through a layer of sICAM-1 expressing cells in an *in vitro* transendothelial migration assay. Thielemann *et al* (50) assessed the concentrations of the sICAM-1 in the serum of female patients with breast cancer. They identified increased concentrations of sICAM-1 in the serum of women with breast cancer compared with the serum of healthy controls (50). In the present study, it was observed that combination of anti-MUC1 antibody with etoposide or OM-86II significantly decreased the level of sICAM1 after 24 and 48 h of incubation in breast cancer cells.

Existing literature has suggested that the addition of monoclonal antibody to chemotherapeutic agents represents a promising strategy in anticancer treatment. The addition of anti-MUC1 antibody to cisplatin or a novel platinum(II) complex resulted in better pro-apoptotic activity and was more efficient than monotherapy in breast cancer cells (15,51). Another previous study showed that anti-MUC1 monoclonal antibody (C595) with docetaxel reduced the tumor burden and ascites in an *in vivo* ovarian cancer model (52). Slamon *et al* (53) demonstrated that the addition of trastuzumab to chemotherapy had more benefits than monotherapy. The final effect of such a treatment was longer survival of patients as well as decreased risk of death (53). The role of MUC1 in resistance to trastuzumab (Herceptin) is well documented (35,54). Fessler *et al* (35) noticed that cancer cells, which exhibit Herceptin resistance, were also resistant to doxorubicin and cyclophosphamide. The resistance to these chemotherapeutic agents was decreased by the combination of the original drug and MUC1 inhibitor (35).

The present study demonstrated that combination therapy based on anti-MUC1 antibody and a novel diisoquinoline derivative (OM-86II) inhibited the proliferation of breast cancer cells. Its inhibitory effects were associated with induction of cell cycle arrest and apoptosis. Moreover, such a combination was able to block the multiple intracellular signaling pathways responsible for tumor growth promotion and breast cancer progression. It was demonstrated that anti-MUC1 antibody with OM-86II decreased the concentration of MMP-2, MMP-9, sICAM1 and mTOR. In addition, combined therapy exhibited anti-inflammatory activity; decreased concentrations of pro-inflammatory cytokine TNF-α and COX-2 were observed. The present study suggested that the combination of anti-MUC1 with novel OM-86II represents a potential multi-targeted strategy in breast cancer treatment.

Acknowledgements

Not applicable.

Funding

The present study was funded by The National Science Centre (grant no. DEC-2017/01/X/NZ7/01315).

Availability of data and materials

All data generated or analyzed during this study are included in this published article.

Authors' contributions

AG, AB and KB designed the study. AG wrote the manuscript, and performed the experiments and statistical analysis of the data. WS, RC and AS performed the *in vitro* experiments. AB analyzed the results and coordinated the study. ZK analyzed data and described the synthesis process. All authors read and approved the final manuscript.

Ethics approval and consent to participate

Not applicable.

Patient consent for publication

Not applicable.

Competing interests

The authors declare that they have no competing interests.

References

1. Anderson WF, Chatterjee N, Ershler WB and Brawley OW: Estrogen receptor breast cancer phenotypes in the surveillance, epidemiology, and end results database. Breast Cancer Res Treat 76: 27-36, 2002.
2. Cleator SJ, Ahamed E, Coombes R and Palmieri CA: A 2009 update on the treatment of patients with hormone receptor-positive breast cancer. Clin Breast Cancer 9 Suppl 1: S6-S17, 2009.
3. Davies E and Hiscox S: New therapeutic approaches in breast cancer. Maturitas 68: 121-128, 2011.
4. Nath S and Mukherjee P: MUC1: A multifaceted oncoprotein with a key role in cancer progression. Trends Mol Med 20: 332-342, 2014.
5. Krishn SR, Kaur S, Smith LM, Johansson SL, Jain M, Patel A, Gautam SK, Hollingsworth MA, Mandel U, Clausen H, *et al*: Mucins and associated glycan signatures in colon adenoma-carcinoma sequence: Prospective pathological implication(s) for early diagnosis of colon cancer. Cancer Lett 374: 304-314, 2016.

6. Hanson RL and Hollingsworth MA: Functional consequences of differential O-glycosylation of MUC1, MUC4, and MUC16 (downstream effects on signaling). Biomolecules 6: E34, 2016.
7. Cascio S and Finn OJ: Intra- and extra-cellular events related to altered glycosylation of MUC1 promote chronic inflammation, tumor progression, invasion, and metastasis. Biomolecules 6: E39, 2016.
8. Pawłowska N, Gornowicz A, Bielawska A, Surażyński A, Szymanowska A, Czarnomysy R and Bielawski K: The molecular mechanism of anticancer action of novel octahydropyrazino[2,1-a:5,4-a']diisoquinoline derivatives in human gastric cancer cells. Invest New Drugs 36: 970-984, 2018.
9. Gornowicz A, Pawłowska N, Czajkowska A, Czarnomysy R, Bielawska A, Bielawski K, Michalak O, Staszewska-Krajewska O and Kałuża Z: Biological evaluation of octahydropyrazin[2,1-a:5,4-a']diisoquinoline derivatives as potent anticancer agents. Tumour Biol 39: 1010428317701641, 2017.
10. Cuya SM, Bjornsti MA and van Waardenburg RCAM: DNA topoisomerase-targeting chemotherapeutics: What's new? Cancer Chemother Pharmacol 80: 1-14, 2017.
11. Kałuża Z, Bielawski K, Ćwiek R, Niedziejko P and Kaliski P: C2-symmetric hemiaminal ethers and diamines: New ligands for copper-catalyzed desymmetrization of meso-1,2-diols and asymmetric Henry reactions. Tetrahedron Asymmetry 24: 1435-1442, 2013.
12. Carmichael J, DeGraff WG, Gazdar AF, Minna JD and Mitchell JB: Evaluation of a tetrazolium-based semiautomated colorimetric assay: Assessment of radiosensitivity. Cancer Res 47: 943-946, 1987.
13. Czarnomysy R, Surażyński A, Muszynska A, Gornowicz A, Bielawska A and Bielawski K: A novel series of pyrazole-platinum(II) complexes as potential anti-cancer agents that induce cell cycle arrest and apoptosis in breast cancer cells. J Enzyme Inhib Med Chem 33: 1006-1023, 2018.
14. Singh SK, Moretta D, Almaguel F, Wall NR, De León M and De León D: Differential effect of proIGF-II and IGF-II on resveratrol induced cell death by regulating surviving cellular localization and mitochondrial depolarization in breast cancer cells. Growth Factors 25: 363-372, 2007.
15. Gornowicz A, Bielawska A, Czarnomysy R, Gabryel-Porowska H, Muszyńska A and Bielawski K: The combined treatment with novel platinum(II) complex and anti-MUC1 increases apoptotic response in MDA-MB-231 breast cancer cells. Mol Cell Biochem 408: 103-113, 2015.
16. Gordon JL, Brown MA and Reynolds MM: Cell-based methods for determination of efficacy for candidate therapeutics in the clinical management of cancer. Diseases 6: E85, 2018.
17. Hugo HJ, Saunders C, Ramsay RG and Thompson EW: New insights on COX-2 in chronic inflammation driving breast cancer growth and metastasis. J Mammary Gland Biol Neoplasia 20: 109-119, 2015.
18. Romieu-Mourez R, François M, Abate A, Boivin MN, Birman E, Bailey D, Bramson JL, Forner K, Young YK, Medin JA and Galipeau J: Mesenchymal stromal cells expressing ErbB-2/neu elicit protective antibreast tumor immunity in vivo, which is paradoxically suppressed by IFN-gamma and tumor necrosis factor-alpha priming. Cancer Res 70: 7742-7747, 2010.
19. Warren MA, Shoemaker SF, Shealy DJ, Bshar W and Ip MM: Tumor necrosis factor deficiency inhibits mammary tumorigenesis and a tumor necrosis factor neutralizing antibody decreases mammary tumor growth in neu/erbB2 transgenic mice. Mol Cancer Ther 8: 2655-2663, 2009.
20. Houghton J, Li H, Fan X, Liu Y, Liu JH, Rao VP, Poutahidis T, Taylor CL, Jackson EA, Hewes C, *et al*: Mutations in bone marrow-derived stromal stem cells unmask latent malignancy. Stem Cells Dev 19: 1153-1166, 2010.
21. Sangaletti S, Tripodo C, Ratti C, Piconese S, Porcasi R, Salcedo R, Trinchieri G, Colombo MP and Chiodoni C: Oncogene-driven intrinsic inflammation induces leukocyte production of tumor necrosis factor that critically contributes to mammary carcinogenesis. Cancer Res 70: 7764-7775, 2010.
22. Hamaguchi T, Wakabayashi H, Matsumine A, Sudo A and Uchida A: TNF inhibitor suppresses bone metastasis in a breast cancer cell line. Biochem Biophys Res Commun 407: 525-530, 2011.
23. Rubio MF, Werbajh S, Cafferata EG, Quaglino A, Coló GP, Nojek IM, Kordon EC, Nahmod VE and Costas MA: TNF-alpha enhances estrogen-induced cell proliferation of estrogen-dependent breast tumor cells through a complex containing nuclear factor-kappa B. Oncogene 25: 1367-1377, 2006.
24. Rivas MA, Tkach M, Beguelin W, Proietti CJ, Rosemblit C, Charreau EH, Elizalde PV and Schillaci R: Transactivation of ErbB-2 induced by tumor necrosis factor alpha promotes NF-kappaB activation and breast cancer cell proliferation. Breast Cancer Res Treat 122: 111-124, 2010.
25. Rivas MA, Carnevale RP, Proietti CJ, Rosemblit C, Beguelin W, Salatino M, Charreau EH, Frahm I, Sapia S, Brouckaert P, *et al*: TNF alpha acting on TNFR1 promotes breast cancer growth via p42/P44 MAPK, JNK, Akt and NF-kappa B-dependent pathways. Exp Cell Res 314: 509-529, 2008.
26. Saal LH, Johansson P, Holm K, Gruvberger-Saal SK, She QB, Maurer M, Koujak S, Ferrando AA, Malmström P, Memeo L, *et al*: Poor prognosis in carcinoma is associated with a gene expression signature of aberrant PTEN tumor suppressor pathway activity. Proc Natl Acad Sci USA 104: 7564-7569, 2007.
27. Engelman JA: Targeting PI3K signalling in cancer: Opportunities, challenges and limitations. Nat Rev Cancer 9: 550-562, 2009.
28. Ciruelos Gil EM: Targeting the PI3K/AKT/mTOR pathway in estrogen receptor-positive breast cancer. Cancer Treat Rev 40: 862-871, 2014.
29. Horm TM and Schroeder JA: MUC1 and metastatic cancer: Expression, function and therapeutic targeting. Cell Adh Migr 7: 187-198, 2013.
30. Shen Q, Rahn JJ, Zhang J, Gunasekera N, Sun X, Shaw AR, Hendzel MJ, Hoffman P, Bernier A and Hugh JC: MUC1 initiates Src-CrkLRac1/Cdc42-mediated actin cytoskeletal protrusive motility after ligating intercellular adhesion molecule-1. Mol Cancer Res 6: 555-567, 2008.
31. Sachdeva M and Mo YY: MicroRNA-145 suppresses cell invasion and metastasis by directly targeting mucin 1. Cancer Res 70: 378-387, 2010.
32. Wei X, Xu H and Kufe D: MUC1 oncoprotein stabilizes and activates estrogen receptor alpha. Mol Cell 21: 295-305, 2006.
33. Woo JK, Choi Y, Oh SH, Jeong JH, Choi DH, Seo HS and Kim CW: Mucin 1 enhances the tumor angiogenic response by activation of the AKT signaling pathway. Oncogene 31: 2187-2198, 2012.
34. Mikami Y, Hisatsune A, Tashiro T, Isohama Y and Katsuki H: Hypoxia enhances MUC1 expression in a lung adenocarcinoma cell line. Biochem Biophys Res Commun 379: 1060-1065, 2009.
35. Fessler SP, Wotkowicz MT, Mahanta SK and Bamdad C: MUC1* is a determinant of trastuzumab (Herceptin) resistance in breast cancer cells. Breast Cancer Res Treat 118: 113-124, 2009.
36. Pillai K, Pourgholami MH, Chua TC and Morris DL: MUC1 as a potential target in anticancer therapies. Am J Clin Oncol 38: 108-118, 2015.
37. Etti IC, Abdullah R, Kadir A, Hashim NM, Yeap SK, Imam MU, Ramli F, Malami I, Lam KL, Etti U, *et al*: The molecular mechanism of the anticancer effect of Artonin E in MDA-MB 231 triple negative breast cancer cells. PLoS One 12: e0182357, 2017.
38. Kim SH, Turnbull J and Guimond S: Extracellular matrix and cell signalling: The dynamic cooperation of integrin, proteoglycan and growth factor receptor. J Endocrinol 209: 139-151, 2011.
39. Walker C, Mojares E and Del Río Hernández A: Role of extracellular matrix in development and cancer progression. Int J Mol Sci 19: E3028, 2018.
40. Jena MK and Janjanam J: Role of extracellular matrix in breast cancer development: A brief update. Version 2 F1000Res 7: 274, 2018.
41. Fingleton B: Matrix metalloproteinases: Roles in cancer and metastasis. Front Biosci 11: 479-491, 2006.
42. Leppä S, Saarto T, Vehmanen L, Blomqvist C and Elomaa I: A high serum matrix metalloproteinase-2 level is associated with an adverse prognosis in node-positive breast carcinoma. Clin Cancer Res 10: 1057-1063, 2004.
43. Huang H: Matrix metalloproteinase-9 (MMP-9) as a cancer biomarker and MMP-9 biosensors: Recent advances. Sensors (Basel) 18: E3249, 2018.
44. Pellikainen JM, Ropponen KM, Kataja VV, Kellokoski JK, Eskelinen MJ and Kosma VM: Expression of matrix metalloproteinase (MMP)-2 and MMP-9 in breast cancer with a special reference to activator protein-2, HER2, and prognosis. Clin Cancer Res 10: 7621-7628, 2004.
45. Di Cara G, Marabeti MR, Musso R, Riili I, Cancemi P and Pucci Minafra I: New insights into the occurrence of matrix metalloproteases -2 and -9 in a cohort of breast cancer patients and proteomic correlations. Cells 7: E89, 2018.

46. Katanov C, Lerrer S, Liubomirski Y, Leider-Trejo L, Meshel T, Bar J, Feniger-Barish R, Kamer I, Soria-Artzi G, Kahani H, *et al*: Regulation of the inflammatory profile of stromal cells in human breast cancer: Prominent roles for TNF-α and the NF-κB pathway. Stem Cell Res Ther 6: 87, 2015.
47. Hosseini F, Hassannia H, Mahdian-Shakib A, Jadidi-Niaragh F, Enderami SE, Fattahi M, Anissian A, Mirshafiey A and Kokhaei P: Targeting of crosstalk between tumor and tumor microenvironment by β-D mannuronic acid (M2000) in murine breast cancer model. Cancer Med 6: 640-650, 2017.
48. Miller TW, Rexer BN, Garrett JT and Arteaga CL: Mutations in the phosphatidylinositol 3-kinase pathway: Role in tumor progression and therapeutic implications in breast cancer. Breast Cancer Res 13: 224, 2011.
49. Rahn JJ, Chow JW, Horne GJ, Mah BK, Emerman JT, Hoffman P and Hugh JC: MUC1 mediates transendothelial migration in vitro by ligating endothelial cell ICAM-1. Clin Exp Metastasis 22: 475-483, 2005.
50. Thielemann A, Baszczuk A, Kopczyński Z, Nowak A and Grodecka-Gazdecka S: The clinical usefulness of assessing the concentration of cell adhesion molecules sVCAM-1 and sICAM-1 in the serum of women with primary breast cancer. Contemp Oncol (Pozn) 18: 252-259, 2014.
51. Gornowicz A, Kałuża Z, Bielawska A, Gabryel-Porowska H, Czarnomysy R and Bielawski K: Cytotoxic efficacy of a novel dinuclear platinum(II) complex used with anti-MUC1 in human breast cancer cells. Mol Cell Biochem 392: 161-174, 2014.
52. Wang L, Chen H, Pourgholami MH, Beretov J, Hao J, Chao H, Perkins AC, Kearsley JH and Li Y: Anti-MUC1 monoclonal antibody (C595) and docetaxel markedly reduce tumor burden and ascites, and prolong survival in an in vivo ovarian cancer model. PLoS One 6: e24405, 2011.
53. Slamon DJ, Leyland-Jones B, Shak S, Fuchs H, Paton V, Bajamonde A, Fleming T, Eiermann W, Wolter J, Pegram M, *et al*: Use of chemotherapy plus a monoclonal antibody against HER2 for metastatic breast cancer that overexpresses HER2. N Engl J Med 344: 783-792, 2001.
54. Raina D, Uchida Y, Kharbanda A, Rajabi H, Panchamoorthy G, Jin C, Kharbanda S, Scaltriti M, Baselga J and Kufe D: Targeting the MUC1-C oncoprotein downregulates HER2 activation and abrogates trastuzumab resistance in breast cancer cells. Oncogene 33: 3422-3431, 2014.